Experimental evidence, numerics, and theory of vibrational resonance in bistable systems

J. P. Baltanás,[1] L. López,[1] I. I. Blechman,[2] P. S. Landa,[3] A. Zaikin,[4] J. Kurths,[4] and M. A. F. Sanjuán[1]
[1]*Nonlinear Dynamics and Chaos Group, Departamento de Matemáticas y Física Aplicadas y Ciencias de la Naturaleza, Universidad Rey Juan Carlos, Tulipán s/n, 28933 Móstoles, Madrid, Spain*
[2]*Mechanobr-Tekhnika Corporation, 22 Liniya, 3, V.O., 1999106 St. Petersburg, Russia*
[3]*Department of Physics, Lomonosov Moscow State University, 119899 Moscow, Russia*
[4]*Nonlinear Dynamics, Institute of Physics, University of Potsdam, Am Neuen Palais 10, 14469 Potsdam, Germany*
(Received 21 November 2002; published 27 June 2003)

We consider an overdamped bistable oscillator subject to the action of a biharmonic force with very different frequencies, and study the response of the system when the parameters of the high-frequency force are varied. A resonantlike behavior is obtained when the amplitude or the frequency of this force is modified in an experiment performed by means of an analog circuit. This behavior, confirmed by numerical simulations, is explained on the basis of a theoretical approach.

DOI: 10.1103/PhysRevE.67.066119 PACS number(s): 05.90.+m, 05.40.−a, 05.45.−a

I. INTRODUCTION

During the last three decades, investigation of signal processing in nonlinear systems in the presence of noise has revealed several intriguing phenomena. One of the most counterintuitive examples of these phenomena is the effect of stochastic resonance (SR), which was initially found in bistable systems [1], and it has been confirmed in a large variety of different dynamical [2–4] and nondynamical systems [5,4], seeming to be recurrent in biological systems (e.g., see Refs. [6–12]). Its basic effect consists in the fact that an optimal quantity of noise, added to the driving signal, improves its detection by a nonlinear system. The very general phenomenon of SR appears in the processing of harmonic [13–15] and aperiodic signals [16–19] by nonlinear systems. Different kinds of noise have been used in order to improve the signal processing such as white noise and colored noise [20–22]. Furthermore, similar effects have been found as well when a chaotic signal is used instead of noise [23].

Another related phenomenon has been described recently [24], where a resonant behavior in a bistable potential with respect to a low-frequency force appears. This phenomenon, called *vibrational resonance* (VR), closely resembles SR although here, a high-frequency harmonic signal plays the role of noise. Besides the case of the bistable potential considered in Ref. [24], the phenomenon of VR has also been found in a spatially extended system where the collective behavior of individual units gives rise to an effective bistable potential, due to the action of multiplicative noise [25].

There is an essential difference between SR and VR. In the first case, noise changes both the effective stiffness and the damping factor of the system, whereas in the latter case the high-frequency vibration changes only the effective stiffness. This can be explained by the fact that in the first case, the third moment of the noise force of the resulting signal is different from zero whereas in the second one, the amplitude to the cube of the high-frequency force is equal to zero [26].

In VR, a bistable system is under the action of a biharmonic perturbation with very different frequencies. It is worth noticing that two-frequency signals are important for communication, since usually a low-frequency signal modulates a high-frequency carrier signal, and is also an object of interest in several other fields such as acoustics [27], neuroscience [28], laser physics [29], or engineering. Engineering constructions can be very sensitive to external perturbations and it is often assumed that this danger exists if the frequency coincides with one of the natural frequencies of the constructions. Our study shows that this is not necessarily the case, as it is indeed possible that frequencies far from them can also cause resonance phenomena.

The goal of this paper is to compare analytical, numerical, and experimental results, related to VR, in a bistable potential driven by two forcing terms, one with a low frequency and the other with a high one. We start with the development of a theoretical approach which explains the phenomena described here. Later, we carry out some numerical simulations and compare the results with the ones given by the theory and the experimental measurements that, as far as we know, have been obtained using a nonlinear electronic circuit for the first time in this work. Our experimental results confirm the appearance of a resonant behavior in the response of the system, both with respect to the amplitude and frequency of the high-frequency component of the biharmonic signal. Finally, we discuss some effects of additive noise on the behavior of this system.

II. DESCRIPTION OF THE MODEL AND THEORETICAL APPROACH TO VR

As the starting point in this paper, we consider the model described by the following equation:

$$\dot{x} - ax + bx^3 = A\cos(\omega t) + B\cos(\Omega t + \Theta), \qquad (1)$$

which corresponds to an overdamped bistable Duffing oscillator driven by two harmonic signals of different frequencies. Here, we assume that $\Omega \gg \omega$, i.e., the term $B\cos(\Omega t+\Theta)$ is a high-frequency force with amplitude B and $A\cos(\omega t)$ is a low-frequency signal of amplitude A.

An approximate solution of this equation, by using the method described in Ref. [30], is given in Refs. [31,32].

According to this method, and for the case of general values of the parameters a and b of the restoring force, we look for a solution in the form

$$x(t)=X(t)+\Psi(t,\Omega t), \tag{2}$$

where $X(t)$ is the variable describing the slow motion component of the response and $\Psi(t,\Omega t)$ is a 2π-periodic function of the "fast" time $\tau=\Omega t$, with zero mean with respect to this time

$$\overline{\Psi(t,\tau)}=\frac{1}{2\pi}\int_0^{2\pi}\Psi(t,\tau)d\tau=0. \tag{3}$$

Starting from Eqs. (2) and (3), it is possible to obtain the following evolution equations for $X(t)$ and $\Psi(t,\Omega t)$:

$$\dot{X}-aX+bX^3+3bX\overline{\Psi}^2+b\overline{\Psi}^3=A\cos(\omega t) \tag{4}$$

$$\dot{\Psi}-a\Psi+3bX^2(\Psi-\overline{\Psi})+3bX(\Psi^2-\overline{\Psi}^2)+b(\Psi^3-\overline{\Psi}^3) =B\cos(\Omega t+\Theta). \tag{5}$$

Remembering that Ψ is a rapidly changing force, we can expect to find that

$$\dot{\Psi}\gg\Psi,\Psi^2,\Psi^3, \tag{6}$$

thus obtaining an approximate evolution equation for the fast part of the motion [Eq. (5)]

$$\dot{\Psi}=B\cos(\Omega t+\Theta). \tag{7}$$

This equation can be trivially solved, leading to

$$\Psi=\frac{B}{\Omega}\sin(\Omega t+\Theta). \tag{8}$$

Now we use this result to find the differential equation governing the slow component of the motion $X(t)$ within this approximation. Taking into account that $\overline{\Psi}^3=0$ and $\overline{\Psi}^2=1/2(B^2/\Omega^2)$, Eq. (4) becomes

$$\dot{X}-aX+bX^3+\frac{3}{2}b\frac{B^2}{\Omega^2}X=A\cos(\omega t). \tag{9}$$

For convenience, we write this expression in the following form:

$$\dot{X}-\hat{a}(B)X+bX^3=A\cos(\omega t), \tag{10}$$

where

$$\hat{a}(B)=a-\frac{3}{2}b\frac{B^2}{\Omega^2}. \tag{11}$$

Equation (10) can be understood as the forced motion of a particle in the effective bistable potential

$$V(X)=-\hat{a}(B)\frac{X^2}{2}+b\frac{X^4}{2}. \tag{12}$$

An analysis of $V(X)$ shows that two different situations, depending on the sign of $\hat{a}(B)$, may be found. If $\hat{a}(B)>0$, the potential has two minima [situated in $X=\pm\sqrt{\hat{a}(B)/b}$] and a maximum (in $X=0$), i.e., we have a typical double-well potential. However, if $\hat{a}(B)\leqslant 0$, we have a single minimum situated in $X=0$, and consequently, the potential is monostable. Coming back to the parameters of our original problem, we can write

$$\text{if } B\geqslant\sqrt{\frac{2a}{3b}}\Omega \text{ we have one minimum in 0,} \tag{13}$$

$$\text{if } B<\sqrt{\frac{2a}{3b}}\Omega \text{ we have two minima in } \pm\sqrt{\hat{a}(B)/b}. \tag{14}$$

Then, the high-frequency component, which is equivalent to noise in SR, induces a bifurcation in the system, whose principal effect consists in changing the number of equilibrium points in the effective potential from two to one as B increases. We will show in the following sections that the origin of the resonant behavior discussed in this paper is closely related to this change in the shape of the effective potential.

In order to analyze in detail the referred bifurcation, let us consider first the situation corresponding to Eq. (14). In this case, we have two equilibrium points situated in

$$X_{1,2}=\pm\sqrt{\frac{a}{b}-\frac{3}{2}\left(\frac{B}{\Omega}\right)^2}. \tag{15}$$

We are interested in obtaining the equation for the deviation of the response X apart from each one of the minima $X_{1,2}$. Following this idea, we write $Y=X-X_{1,2}$ and substitute this quantity in Eq. (10), thus getting, after some algebraic manipulations,

$$\dot{Y}+2\hat{a}(B)Y+bY^3+3bX_{1,2}Y^2=A\cos(\omega t). \tag{16}$$

Assuming that our system evolves near one of the equilibrium points and that the deviations from the equilibrium points are small ($A\ll 1$ and $t\to\infty$), linearization of this equation results in

$$\dot{Y}+k(B)Y=A\cos(\omega t), \tag{17}$$

where we have written $k(B)=2\hat{a}(B)$. Using standard methods, we define a parameter Q as the ratio of the amplitude of the low-frequency output oscillations, governed by Eq. (17) within our approximation, to the amplitude of the low-frequency forcing A. In this case Q becomes

$$Q=\frac{1}{\sqrt{k^2+\omega^2}}=\frac{1}{\sqrt{\omega^2+4\left(a-\dfrac{3bB^2}{2\Omega^2}\right)^2}}, \tag{18}$$

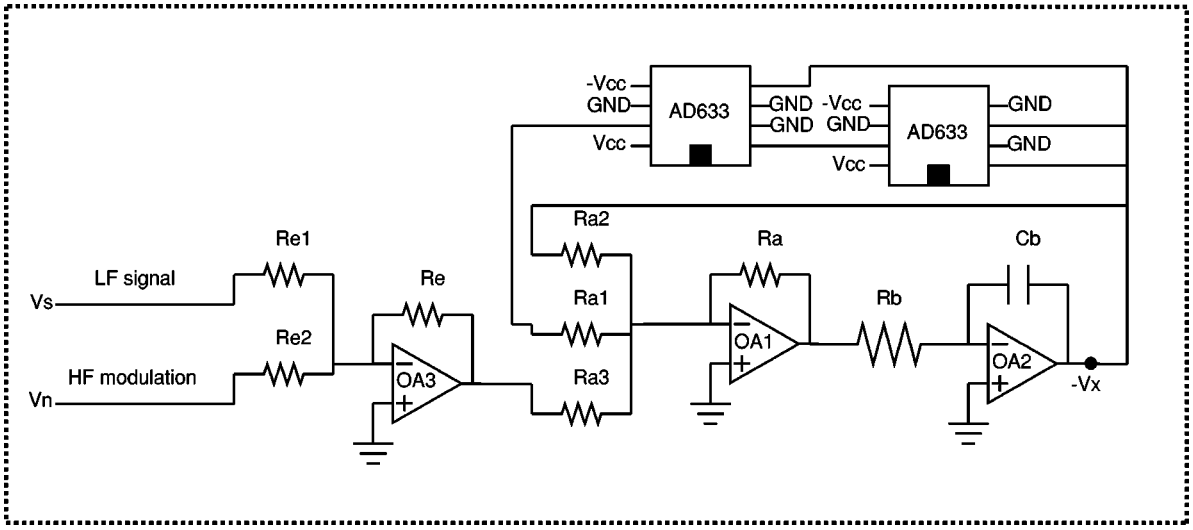

FIG. 1. Circuit used in the analog simulations of the overdamped Duffing oscillator. The use of the parameter values given in the text gives rise to a double-well potential with a separation between minima equal to $L=2$ and a barrier height $H=9.3$.

whereas the phase shift ψ is given by

$$\psi = -\arctan\left(-\frac{\omega}{k}\right). \tag{19}$$

Analogously, we can write the equation for the deviation of X from the equilibrium point in the case described in Eq. (13), where we have a single minimum situated in $X_0=0$. It is straightforward to see that after linearization under the same conditions given above, the equation obeyed by Y reads

$$\dot{Y} - \hat{a}(B)Y = A\cos(\omega t), \tag{20}$$

which is exactly Eq. (17) where $k(B)$ is changed by $-\hat{a}(B)$. Then, the response and phase shift are given by Eqs. (18) and (19), where we write $-\hat{a}(B)$ instead of $k(B)$. In particular,

$$Q = \frac{1}{\sqrt{\omega^2 + \left(a - \dfrac{3bB^2}{2\Omega^2}\right)^2}}. \tag{21}$$

Let us write the solutions for the deviations Y obtained above, in both cases (two and one equilibrium points) in terms of the parameters of the high-frequency forcing signal, i.e., its amplitude B and frequency Ω. Let us suppose also that we fix the value of the forcing frequency. Then, for a given bistable potential (a and b fixed), Q increases if $B < \sqrt{2a/3b}\,\Omega$ when B increases [Eq. (18)] and decreases if $B > \sqrt{2a/3b}\,\Omega$ when B increases [Eq. (21)]. As Q gives us an idea about the amplitude of the slow component of the output of the system in relation to the amplitude of low-frequency input, this means that a resonance occurs in the system when

$$B = \sqrt{\frac{2a}{3b}}\,\Omega, \tag{22}$$

which corresponds to the critical value of the effective stiffness parameter ($\hat{a}=0$) where the renormalized potential changes its number of equilibrium points from two to one. It is not difficult to see that a similar behavior can be obtained if we fix the amplitude B and change the high frequency Ω. This point will be confirmed also by the numerical simulations and experiments presented in the following section.

III. NUMERICAL AND EXPERIMENTAL RESULTS

One main point in this paper is the experimental confirmation of the theory presented in the preceding section. In particular, we will focus our attention in the experimental evaluation of the response parameter Q. To this end, we have used the electronic circuit shown in Fig. 1.

It is composed of three LM741 operational amplifiers, two AD633 analog multipliers, one capacitor, and eight resistors. In order to minimize the effect of parasitic noise, the circuit has been designed with a minimum number of components. Similar circuits have been already described in the literature in order to analyze some phenomena related to stochastic resonance [33].

Functionally, the circuit consists of two main parts. The first one (operational amplifier OA3 and resistors R_e, R_{e1}, and R_{e2}) is an adder, whose function is to add the low- and high-frequency signals. The second part is the integrator in the double-well potential, which consists of another adder (R_a, R_{a1}, R_{a2}, R_{a3}, and the operational amplifier OA1), two multipliers (AD633 with coefficient α) and an integrator (R_b, C_b, and the operational amplifier OA2). This whole circuit implements the dynamical equation of an overdamped double-well Duffing oscillator of the form

$$R_bC_b\dot{V}_x = V_x\frac{R_a}{R_{a2}} - V_x^3\alpha^2\frac{R_a}{R_{a1}} + V_s\frac{R_aR_e}{R_{a3}R_{e1}} + V_n\frac{R_aR_e}{R_{a3}R_{e2}}, \tag{23}$$

where $-V_x$ is the voltage at the output of the operational

amplifier OA2, V_s is the low-frequency signal, and V_n is the high-frequency modulation [compare with Eq. (1)].

We have chosen the following set of values for the resistors and the capacitor: $R_a=56\ \mathrm{K}\Omega$, $R_{a1}=150\ \Omega$, $R_{a2}=15\ \mathrm{K}\Omega$, $R_{a3}=22\ \mathrm{K}\Omega$, $R_e=2.2\ \mathrm{K}\Omega$, $R_{e1}=6.7\ \mathrm{K}\Omega$, $R_{e2}=2.2\ \mathrm{K}\Omega$, $R_b=10\ \mathrm{K}\Omega$, and $C_b=10\ \mu\mathrm{F}$. The resistors and the capacitor, both have a tolerance of 5%. These parameter values lead to a dynamical equation for the circuit similar to that of a conventional symmetric double-well potential system with a separation between the minima equal to $L=2$ and a barrier height $H=9.3$. The reason for using these parameters instead of a and b is that in our experimental setup, it is easier to change the barrier height H and the separation between minima L of the bistable potential than constants a and b themselves. Both pairs of constants are related to each other through the expressions

$$a=\frac{16H}{L^2},\quad b=\frac{64H}{L^4}. \tag{24}$$

The low-frequency signal V_s and the high-frequency modulation V_n have been generated with two 33120A Agilent wave form generators, and the response V_x of the system has been captured with a Tektronix digital oscilloscope.

Besides the analog experiments, we have carried out numerical simulations of the same system by using a second order Runge-Kutta integration scheme, with a time step of $\Delta t=2.5\times10^{-4}$, in order to compare with both the theory and the results obtained from the circuit. The same values $H=9.3$ and $L=2$ used in the experiment have also been used in the numerical simulations.

Following Ref. [24], we have calculated experimentally and numerically the response of the system, defined by

$$Q=\sqrt{B_c^2+B_s^2}, \tag{25}$$

where B_c and B_s are the cosine and sine components of the output signal, that is,

$$B_s=\frac{2}{nT}\int_0^{nT}x(t)\sin(\omega t)dt,\quad B_c=\frac{2}{nT}\int_0^{nT}x(t)\cos(\omega t)dt, \tag{26}$$

where $T=2\pi/\omega$ and n is an integer. Notice that the definition of the response given above differs from that of Eqs. (18) and (21). In particular, it must be taken into account that, in order to compare theory and simulations, we need to normalize the results obtained by means of Eq. (25) (by dividing by A), and to multiply the theoretical ones [given by Eqs. (18) and(21)] by a factor of 2 appearing in Eq. (26).

In Fig. 2, we show the numerical and the experimental values for the response [Eq. (25)] of the systems given by Eq. (1) and Eq. (23), respectively, to the varying amplitude of the high-frequency signal (natural frequency equal to 10 Hz), clearly showing a resonant behavior as expected from our theoretical predictions. The different symbols mean different values for the amplitude of the low-frequency signal (natural frequency equal to 0.2). We observe that the experimentally obtained values are somehow displaced to the right

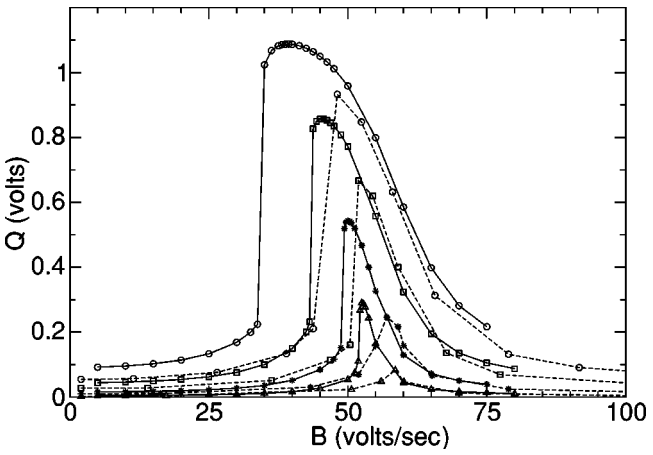

FIG. 2. Numerical and experimental values for response Q (in volts) vs amplitude B of the high-frequency signal. The continuous lines correspond to numerical values, whereas the dashed ones stand for the experiment. The different symbols mean different values for the amplitude of the low-frequency signal: circles, $A=6.656$; squares, $A=3.328$; stars, $A=1.248$; and triangles, $A=0.416$.

and the corresponding responses are a bit smaller than the numerical ones, although the behavior is very similar in both cases. The differences observed among numerical and experimental results could be explained by considering the fact that some components of the experimental circuit (in particular, resistances) could introduce a certain variability in the experimental values of the parameters of the bistable potential (mainly in the barrier height).

In Fig. 3, the numerical values of the normalized response corresponding to the cases of Fig. 2 are depicted and compared with the theoretical approximation given by the theory (see also Refs. [31,32]). Notice that in the evaluation of the theoretical approximation of the response, we must use two

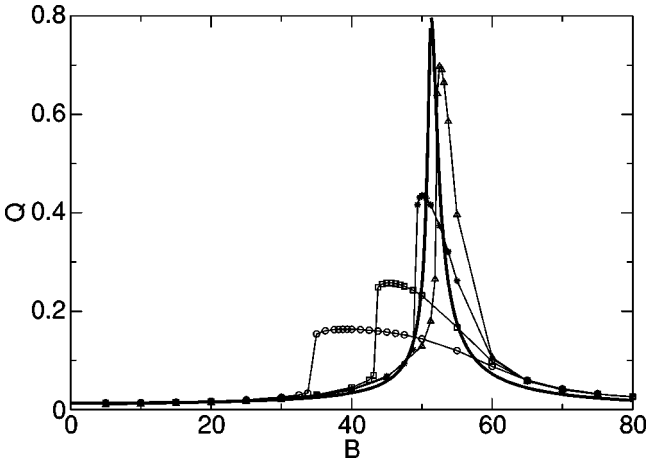

FIG. 3. Numerically calculated values of the system response vs. theory (thick line). Symbols mean the same as in Fig 2. Note that we have normalized the numerical values by dividing by A, and the theoretical ones have been multiplied by a factor of 2 in order to compare numerics and theory. As it is clearly seen, the numerical values tend to the theoretical resonant curve when A is diminished.

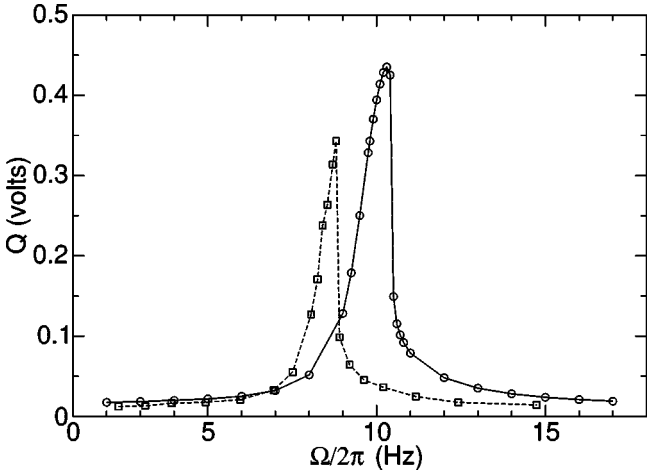

FIG. 4. Resonant behavior of the system with frequency Ω when $\omega/2\pi=0.2$, $A=0.832$, and $B=52.6815$. Circles correspond to numerical simulations and squares to the experiments.

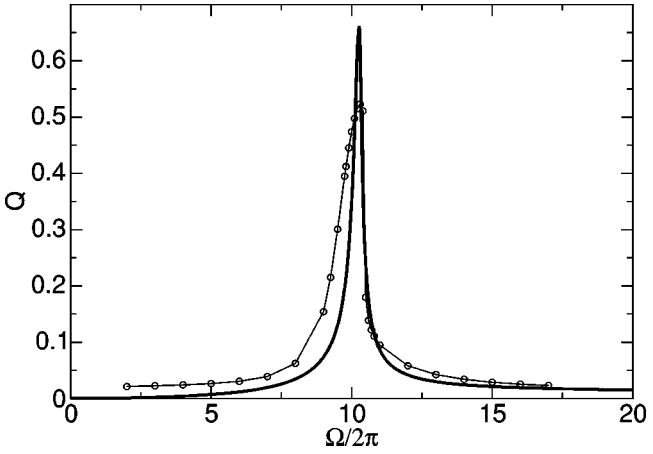

FIG. 5. Theoretical and numerical values for the case of the resonance with the frequency. The values of the parameters are the same as used in Fig. 4.

different expressions of Q, one for the left side of the resonant point, i.e., Eq. (18), and Eq. (21) for the right side. In this figure, it is clear that when the amplitude of the low-frequency signal A is decreased, the value of B for which the maximum is obtained tends to the theoretical one. Indeed, the results suggest that the theory describes properly the observed behavior only for small values of the amplitude of the low-frequency signal A, as expected from the approximation under which the theory has been obtained. Moreover, it can be seen that even for small values of the amplitude A, some differences persist among theory and numerics. The origin of these differences lies in the fact that the linearization is performed on a result that is itself an approximation, i.e., that given by Eqs. (2) and (3) corresponding to the time scale separation.

In Fig. 4 the resonance emerging when $\Omega/2\pi$ (instead of the amplitude) is varied in the high-frequency signal, is shown by means of the experiment and the numerical simulations. The notation is the same as in the previous figure. Here, the experimental curve is shifted towards the left and the values for Q are a bit smaller than those obtained from the numerical simulations, but again the resonant behavior is very similar in both cases. The frequency of the slow signal is again 0.2, but we have chosen an amplitude equal to 0.832. The amplitude for the fast signal is now 52.6815. This value corresponds to the location of the maximum response of the system provided by the theory.

Finally, in Fig. 5, theoretical and numerical results are compared in the same way as before, for the case of the dual resonant curve that results when Ω is varied for a fixed value of B. As observed from the figure, the simulations predict a value for the maximum location, which is rather well estimated by the theory. Nevertheless, the numerical values for Q are smaller than the theoretical ones, as occurred previously.

IV. EFFECTS OF NOISE ON VIBRATIONAL RESONANCE

As is well known, noise can play an important role in the behavior of certain dynamical systems. In particular, the standard bistable potential considered in this work constitutes a paradigm in the study of the effects of noise on nonlinear systems, for example, in the context of SR. So, it seems natural to investigate the action of a certain amount of additive noise on the resonant behavior described above (VR). It should be noted that we do not pretend to explore in detail the effects of noise on VR in this section, but only some of the main consequences of including a stochastic term in our system. In particular, we add white Gaussian noise to the model described by Eq. (1), and get the following equation:

$$\dot{x}-ax+bx^3=A\cos(\omega t)+B\cos(\Omega t+\Theta)+\xi(t), \quad (27)$$

where the moments for the noisy term are

$$\langle\xi(t)\rangle=0, \quad \langle\xi(t)\xi(s)\rangle=D\delta(t-s), \quad (28)$$

D being the intensity of the noise.

We consider first the implications of adding a stochastic term when only the amplitude of the high-frequency force B is varied. We have carried out numerical simulations by using a stochastic version of the Heun algorithm (cf. [34]). The results are depicted in Fig. 6. The first striking effect is that the maximum of the resonance curve diminishes as D increases and, at the same time, its location is shifted towards lower values of the high-frequency amplitude B. This is due to the fact that, in this situation, noise works as a fraction of the high-frequency signal component, thus advancing the resonance. Another interesting result is that the vibrational resonance effect completely disappears for large values of D. The origin of this effect comes from the fact that white noise provides an input to the system with contributions coming from all frequencies. This masks the contribution of the high-frequency signal, and its relative importance in the response of the system is decreased. Of course these two effects will become more and more relevant as D increases. Likewise, it is worth noting that the classical stochastic resonance behavior is recovered precisely when B is 0, as is observed in this

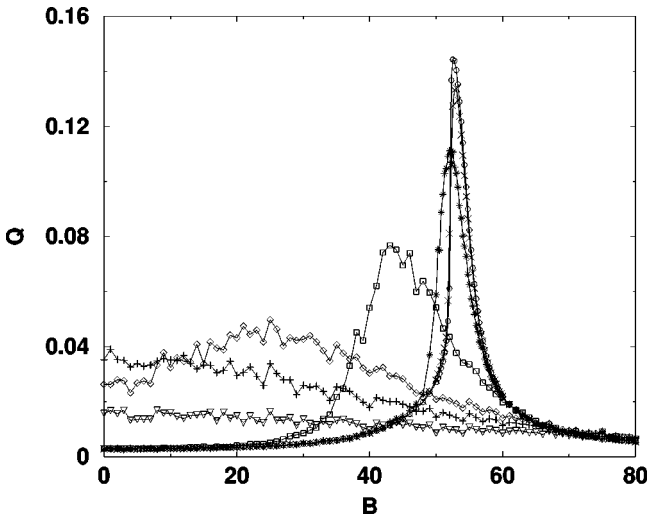

FIG. 6. Response of the forced bistable system in the presence of noise of different intensities. $A=0.416$, $\omega/2\pi=0.2$, and $\Omega/2\pi=10$. The meanings of the symbols are: circles $D=0.0001$, crosses $D=0.01$, stars $D=0.1$, squares $D=1$, diamonds $D=5$, plus signs $D=10$, and triangles down $D=30$. Note that the noise broadens the response curve of the system and advances the value of B that gives the maximum response at the same time as these maximal values diminishes. The conventional SR effect is clearly seen for $B=0$.

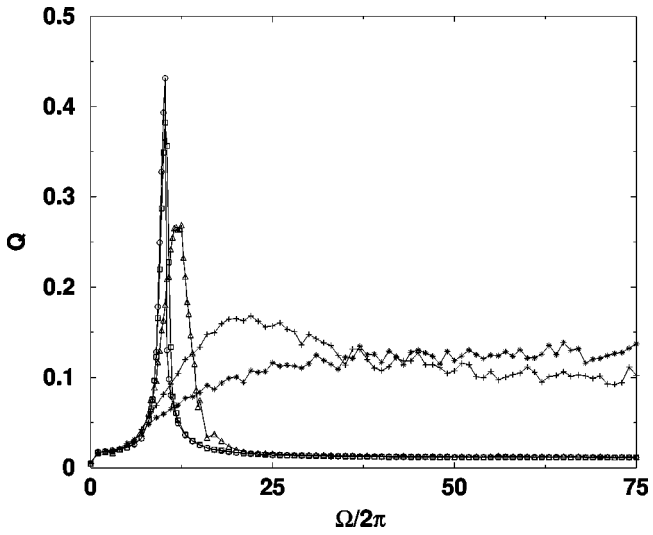

FIG. 7. Response of the forced bistable system in the presence of noise when the high frequency is varied. $A=0.832$, $B=52.6825$, and $\omega/2\pi=0.2$. The meanings of the symbols are: circles $D=0.001$, squares $D=0.1$, triangles $D=1$, plus signs $D=5$, and stars $D=10$.

figure. This means that response Q of the system passes through a maximum as D is increased.

The frequency resonant behavior that we have reported in the preceding section is also modified in the presence of noise. To show this, we have fixed the amplitudes of both the high- and the low-frequency signals and have computed the response Q of the system when Ω is varied for different values of the noise intensity D. The results are drawn in Fig. 7. This phenomenon is similar to the one found when B is varied. In both cases, the maximum of the response curve decreases as D increases. Additionally, for high enough values of D, there is no more resonance effect with respect to the frequency (see Fig. 7).

V. CONCLUSIONS

We have discussed the phenomenon of vibrational resonance in a bistable system under the action of a two-frequency signal with one frequency much larger than the other one. Changing the amplitude of the high-frequency component improves signal processing of the low frequency in a resonant way. First the response of the system is increased and then decreased. Additionally, resonant behavior in the response of the system is also observed with respect to the high frequency, demonstrating two different but related resonances. We have compared analytical, experimental, and numerical results, and found a good matching. To our knowledge, this is the first experimental evidence of the phenomenon of vibrational resonance described in the literature. Finally, we have studied the influence of white noise on VR in bistable systems, showing that noise can advance VR and, at the same time, decrease the resonant effect.

We hope that our theoretical, experimental, and numerical findings will stimulate further work on VR in different kinds of systems. The potential applications of these phenomena include neuronal dynamics, communications technologies, and mechanical engineering.

ACKNOWLEDGMENTS

J. P. Baltanás would like to thank Dr. J. Casado-Pascual for his critical reading of the manuscript and fruitful discussions. P. Landa acknowledges a research stay at the Universidad Rey Juan Carlos, where this work was thoroughly discussed. J. P. Baltanás, L. López, and M. A. F. Sanjuán thank the Spanish Ministry of Science and Technology (Project BFM2000-0967), A.Z. the Microgravity Application Program/Biotechnology of the European Space Agency (ESA), and J.K. the SFB 555 (Germany) for support.

[1] R. Benzi, A. Sutera, and A. Vulpiani, J. Phys. A **14**, L453 (1981).
[2] K. Wiesenfeld and F. Moss, Nature (London) **373**, 33 (1995).
[3] L. Gammaitoni, P. Hänggi, P. Jung, and F. Marchesoni, Rev. Mod. Phys. **70**, 223 (1998).
[4] V. Anishchenko, A. Neiman, F. Moss, and L. Schimansky-Geier, Phys. Usp. **42**, 7 (1999).
[5] J. Vilar, G. Gomila, and J. Rubí, Phys. Rev. Lett. **81**, 14 (1998).
[6] J. Douglass, L. Wilkens, E. Pantazelou, and F. Moss, Nature (London) **365**, 337 (1993).
[7] E. Pantazelou, C. Dames, F. Moss, J. Douglass, and L. Wilkens, Int. J. Bifurcation Chaos Appl. Sci. Eng. **5**, 101 (1995).

[8] P. Cordo, J. Inglis, S. Verschueren, J. Collins, D. Merfeld, S. Rosenblum, S. Buckley, and F. Moss, Nature (London) **383**, 769 (1996).
[9] J.J. Collins, T.T. Imhoff, and P. Grigg, Phys. Rev. E **56**, 923 (1997).
[10] K.A. Richardson, T.T. Imhoff, P. Grigg, and J.J. Collins, Chaos **8**, 599 (1998).
[11] D. Russell, L. Wilkens, and F. Moss, Nature (London) **402**, 291 (1999).
[12] T. Mori and S. Kai, Phys. Rev. Lett. **88**, 218101 (2002).
[13] P. Jung and P. Hanggi, Europhys. Lett. **8**, 505 (1989).
[14] P. Jung, Z. Phys. B: Condens. Matter **76**, 521 (1989).
[15] L. Gammaitoni, E. Menichella-Saetta, S. Santucci, F. Marchesoni, and C. Presilla, Phys. Rev. A **40**, 2105 (1989).
[16] J.J. Collins, C.C. Chow, and T.T. Imhoff, Phys. Rev. E **52**, 3321 (1995).
[17] J.J. Collins, C.C. Chow, A.C. Capella, and T.T. Imhoff, Nature (London) **383**, 770 (1996).
[18] C.C. Chow, T.T. Imhoff, and J.J. Collins, Chaos **8**, 616 (1998).
[19] S. Barbay, G. Giacomelli, and F. Marin, Phys. Rev. Lett. **85**, 4652 (2000).
[20] A. Neiman and L. Schimansky-Geier, Phys. Rev. Lett. **72**, 2988 (1994).
[21] A. Neiman and W. Sung, Phys. Lett. A **223**, 341 (1996).
[22] D. Nozaki, D.J. Mar, P. Grigg, and J.J. Collins, Phys. Rev. Lett. **82**, 2402 (1999).
[23] S. Sinha, Physica A **270**, 204 (1999).
[24] P. Landa and P. McClintock, J. Phys. A **33**, L433 (2000).
[25] A.A. Zaikin, L. López, J.P. Baltanás, J. Kurths, and M.A.F. Sanjuán, Phys. Rev. E **66**, 011106 (2002).
[26] P. Landa, *Regular and Chaotic Oscillations* (Springer-Verlag, Berlin, 2001).
[27] A. Maksimov, Ultrasonics **35**, 79 (1997).
[28] J. Victor and M. Conte, Visual Neurosci. **17**, 959 (2000).
[29] D. Su, M. Chiu, and C. Chen, J. Soc. Precis. Eng. **18**, 161 (1996).
[30] I.I. Blechman, *Vibrational Mechanics* (World Scientific, Singapore, 2000).
[31] I.I. Blekhman and P.S. Landa, Prikladnaya Nelineynaya Dinamika **10**, 44 (2002).
[32] I.I. Blekhman and P.S. Landa, Int. J. of Non-Linear Mech. (to be published).
[33] *Nonlinear Dynamics in Circuits*, edited by T. Carroll and L. Pecora (World Scientific, Singapore, 1995).
[34] J. García-Ojalvo and J.M. Sancho, *Noise in Spatially Extended Systems* (Springer, New York, 1999).